Narrow heavy-hole cyclotron resonances split by the cubic Rashba spin-orbit interaction in strained germanium quantum wells

M. Failla, M. Myronov, C. Morrison, D. R. Leadley, and J. Lloyd-Hughes*
University of Warwick, Department of Physics, Gibbet Hill Road, Coventry CV4 7AL, United Kingdom
(Received 15 October 2014; revised manuscript received 1 May 2015; published 14 July 2015)

The spin-orbit interaction was found to split the cyclotron resonance of heavy holes confined in high-mobility, compressively strained germanium quantum wells. The interference between coherent spin-split cyclotron resonances was tracked on picosecond time scales using terahertz time-domain spectroscopy. Analysis in the time domain, or using a time-frequency decomposition based on the Gabor-Morlet wavelet, was necessary when the difference between cyclotron frequencies was comparable to the linewidth. The cubic Rashba spin-orbit coefficient β was determined via two methods: (i) the magnetic-field dependence of the cyclotron frequencies, and (ii) the spin-resolved subband densities. An enhanced β and spin polarization was created by tailoring the strain to enhance the spin-orbit interaction. The amplitude modulation of the narrow, interfering cyclotron resonances is a signature of spin coherences persisting for more than 10 ps.

DOI: 10.1103/PhysRevB.92.045303 PACS number(s): 73.21.−b, 73.63.Hs, 75.76.+j, 76.40.+b

The spin-orbit interaction creates rich and surprising physical effects, such as magnetoelectric coupling between magnetic and ferroelectric order [1,2] and the quantum spin-Hall effect [3,4]. In conductive 2D systems with structural inversion asymmetry the Rashba spin-orbit interaction lifts spin degeneracy without needing an external magnetic field [5,6] and can permit spin field-effect transistors where spin transport is controlled by an electric field [7,8]. Cyclotron resonance (CR) spectroscopy [9,10] can elucidate the physics of such 2D electronic systems by determining the effective mass m^*, sheet carrier density, and Landau level width, independently of dc phenomena such as Shubnikov–de Haas (SdH) oscillations and the Hall effect, and in a contactless manner.

Substantial efforts to develop Ge-based two-dimensional hole gases (2DHGs) for spintronic applications are motivated by its high hole mobility and compatibility with current Si CMOS technology [11–17]. The strain within Ge-QWs lifts the degeneracy at $k = 0$ of light (LH) and heavy hole (HH) bands, leading to occupied HH bands with reduced intervalley scattering and m^* [18]. Spin-orbit coupling due to Dresselhaus spin-orbit coupling (bulk inversion asymmetry) is absent in centrosymmetric bulk Ge, unlike the case for polar III-V materials [19]. Further, HHs ($m_J = \pm 3/2$) exhibit the cubic Rashba interaction, in contrast to the linear Rashba effect present for electrons and LHs ($m_J = \pm 1/2$) [19–21]. A previous study of a Ge-QW (with -2.1% strain) reported a spin-splitting energy $\Delta = 0.3$–0.4 meV (tuned by an electric field) [21], corresponding to a cubic Rashba coefficient $\beta = 0.1$–$0.07 \times 10^{-28}\,\mathrm{eV\,m^3}$.

In this article we report that the cyclotron resonance of heavy holes in high-mobility strained Ge quantum wells is split by the cubic Rashba spin-orbit interaction. A large spin-orbit coefficient and an enhanced degree of spin polarization were obtained using Ge quantum wells with optimized strain. A time-frequency decomposition technique and time-domain fits were utilized, and were particularly important when the splitting energy was comparable to the Landau level width. The persistence of interference between narrow, spin-split cyclotron resonances suggests a spin relaxation time (the lifetime for the decay of spin polarization) exceeding 10 ps.

Si-Ge heterostructures were grown using an ASM Epsilon 2000 RP-CVD reactor. The structure of the samples, labeled SiGe1 (QW thickness $L_{QW} = 11$ nm) and SiGe2 ($L_{QW} = 22$ nm), is reported in Fig. 1(a) of the Supplemental Material [22]. For both samples relaxed $Si_{0.2}Ge_{0.8}$ buffer layers enclosed the strained Ge-QW, and holes were provided by a boron-doped $Si_{0.2}Ge_{0.8}$ supply layers. Low-temperature (0.3 K) transport parameters obtained by resistivity and Hall effect measurements are reported in Table I. High-resolution x-ray diffraction reciprocal space maps found that the QWs in both samples exhibited 0.8% compressive strain with respect to $Si_{0.2}Ge_{0.8}$.

THz time-domain spectroscopy (THz-TDS) [24] facilitates a powerful variant of CR spectroscopy, as the complex magnetoconductivity of 2D systems can be directly determined from coherent oscillations in the electric field [10,25,26]. A THz time-domain spectrometer measured the electric field $E(t)$ of linearly polarized THz pulses transmitted through a sample, which was placed in a superconducting magnet ($B \leqslant 7.5$ T perpendicular to the QWs, 2 K to 300 K). The presented $E(t)$ includes the deconvolution of the 2 mm ZnTe electro-optic detection crystal's response [27]. The experimental time-domain window was limited to 13 ps by the internal reflection of the THz probe pulse in the silicon substrates. As the frequency-domain resolution for this time window is only 0.08 THz we performed a zero-padding/zero-removal method, described in the Supplemental Material [22]. In order to rule out any possible contribution from carriers in the substrates or the supply layers to the observed CR of the 2DHG (obtained at 2 K), CR spectra at elevated temperatures (above 40 K) were obtained [22], which were consistent with the literature for bulk silicon [28].

At 2 K carriers within the substrate cannot be thermally excited, and with a low chemical potential only the HH subband will be populated. The time-domain oscillation in $\Delta E(t) = E(t,B) - E(t,0)$ reported in Fig. 1(a) (colored lines) can therefore be attributed to the CR of HHs within the sGe-QW. A reference sample with just the graded SiGe layer showed no CR at 2 K. In the time domain the damped CR

*j.lloyd-hughes@warwick.ac.uk

TABLE I. 2DHG properties: Well thickness (L_{QW}), hole sheet density (p_s), effective mass (m^*), and Hall mobility (μ_H) as evaluated by magnetotransport (resistivity and Hall) measurements (MT) [23] at 0.3 K and THz-TDS at 2 K (THz).

	L_{QW} (nm)	$p_{s,MT}$ (10^{11} cm^{-2})	$p_{s,THz}$ (10^{11} cm^{-2})	m^*_{MT} (m_0)	m^*_{THz} (m_0)	m^{*a}_b (m_0)	μ_H (10^5 cm^2/V s)
SiGe1	11	5.9	9.7 ± 0.3	0.095	0.115 ± 0.003	0.103	4.5
SiGe2	22	2	3.1 ± 0.4	0.065	0.083 ± 0.005	0.087	7.8

[a]As evaluated by fitting the CR energies using Eq. (2).

oscillation ($t > 1$ ps) can be seen to increase in frequency at higher fields, with a simultaneous reduction in the decay lifetime. The time domain becomes steadily more complex with increasing B, with beating effects that result from multiple interfering CRs. This can be seen readily in the frequency domain [Fig. 1(b)], where multiple CRs are distinctly resolved at $B \geqslant 4.0$ T for SiGe1 and SiGe2. These CRs arise from transitions between occupied $|N\rangle$ and unoccupied $|N+1\rangle$ spin-split Landau levels (LLs), with two CRs when a LL is almost full or empty, or three CRs for partial LL occupancy. This is pictured schematically in Figs. 1(c) and 1(d) for different fill factors $\nu = hp/eB$, where p is the total sheet hole density. The CR absorption in SiGe2 is weaker than in SiGe1, as a result of its lower hole density (Table I).

To obtain time- and frequency-resolved information from the induced cyclotron oscillation ΔE we introduce the Gabor-Morlet wavelet transform $G(\omega,t',\sigma)$, given by

$$G(\omega,t',\sigma) = \int_{-\infty}^{\infty} \Delta E(t) e^{-(t-t')^2/2\sigma^2} e^{i\omega t} dt \qquad (1)$$

for a Gaussian envelope centered at time t' and with width defined by σ. A judicious choice of σ in the range $0.5 < \sigma < 2.5$ ps permits the amplitude of the CR to be examined at time t', at the expense of a poorer frequency resolution. The time-averaged (Fourier) transform is recovered in the limit $\sigma \to \infty$.

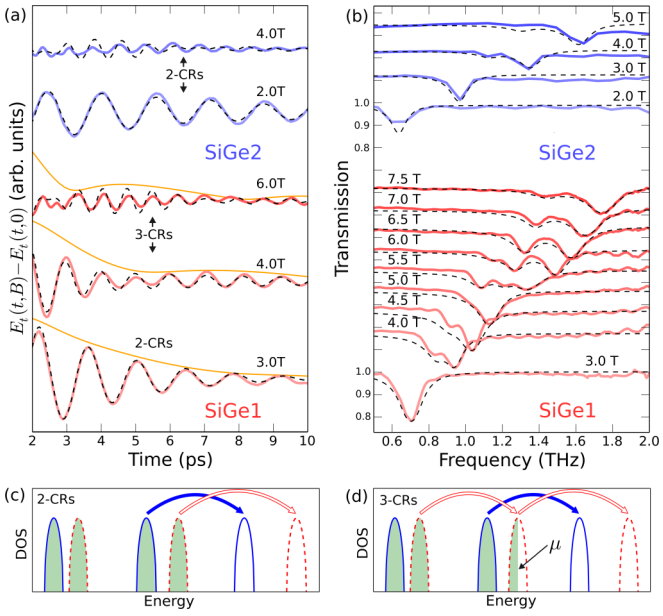

FIG. 1. (Color online) (a) Time-domain cyclotron resonance (CR) $\Delta E = E(t,B) - E(t,0)$ at $T = 2$ K. Solid blue and red lines are experimental data, and dashed lines are fits with two (2 CRs) or three (3 CRs) resonances, as described in the text. For each B the orange lines show the time dependence of the Gabor-Morlet amplitude $|G(\omega,t')|$ at the frequency of the highest spin-split CR. (b) Amplitude of the THz transmission, showing split CRs at $B > 3$ T for both samples. Curves are offset vertically for clarity. Dashed lines were obtained with the parameters from the time-domain fits. (c) Schematic density of states (DOS) at B such that 4 spin-split Landau levels are completely occupied (shaded areas), giving 2 CRs. Solid (dashed) lines denote spin up (down) states. (d) As (c), but for a filling factor ν such that the chemical potential μ is within a Landau level.

In Figs. 2(a) and 2(b) the CR amplitude $|G(\omega,t',\sigma)|$ is reported for SiGe1 at two magnetic fields and at 2 K, and with $\sigma = 1.5$ ps. Two temporal regimes can be distinguished. At early times (below 3 ps) $|G|$ exhibits a broadband response (corresponding to the driving electric field) that develops into a narrow-band cyclotron resonance at later times. At late times ($t' > 3.5$ ps) $|G|$ represents the free-induction decay of the inter-Landau-level transitions.

While multiple resonances can be clearly resolved in the frequency domain in Fig. 2(b) at $B = 5.5$ T, as indicated by the dashed horizontal lines, at $B = 5.0$ T there is no clear splitting either in $|G|$ [Fig. 2(a)] or in the Fourier transform [Fig. 1(b)]. This is because the splitting in the frequency domain is comparable to the linewidths of the CR transitions, and is also the case for $B \leqslant 3.0$ T. In Figs. 2(c) and 2(d) time slices of the Gabor-Morlet amplitude $|G|$ at fixed frequencies are plotted with a logarithmic y axis. The deviation from an exponential decay (dashed lines) indicates that there are multiple, interfering CRs: a single CR would just exhibit an exponential decay with lifetime given by the Landau level width [22]. Thus the Gabor-Morlet waveform provides a sensitive analysis method to examine whether a broad resonance consists of multiple narrower resonances, by permitting beats between spin-split CRs to be observed.

The persistence of interference between spin-up-up and spin-down-down CRs over the experimental time window for all magnetic fields provides direct evidence that the up and down spin populations remain phase-coherent over this time scale, with a spin-relaxation time $\tau_s > 10$ ps. Here, τ_s is the relaxation time associated with the decay in spin polarization. Both the Elliot-Yafet (EY) and the Dyakonov-Perel (DP) spin-relaxation mechanisms may contribute in sGe-QWs [29,30]. Momentum scattering destroys spin coherence in the EY process, which predicts $\tau_s \propto \tau_t/(g^* - g_0)^2$, where g^* is the effective hole g factor, $g_0 = 2.022$, and τ_t is the momentum scattering time [29]. The DP mechanism [30] is also active in systems without inversion symmetry.

Weak antilocalization results [21] reported $\tau_s \sim 16$ ps when $\Delta = 0.30$ meV and $\tau_t = 0.16$ ps, and identified the DP process as dominant. Scaling this value of τ_s according to the DP process ($\tau_s \propto 1/\tau_t$) predicts that $\tau_s < 0.2$ ps for the values of

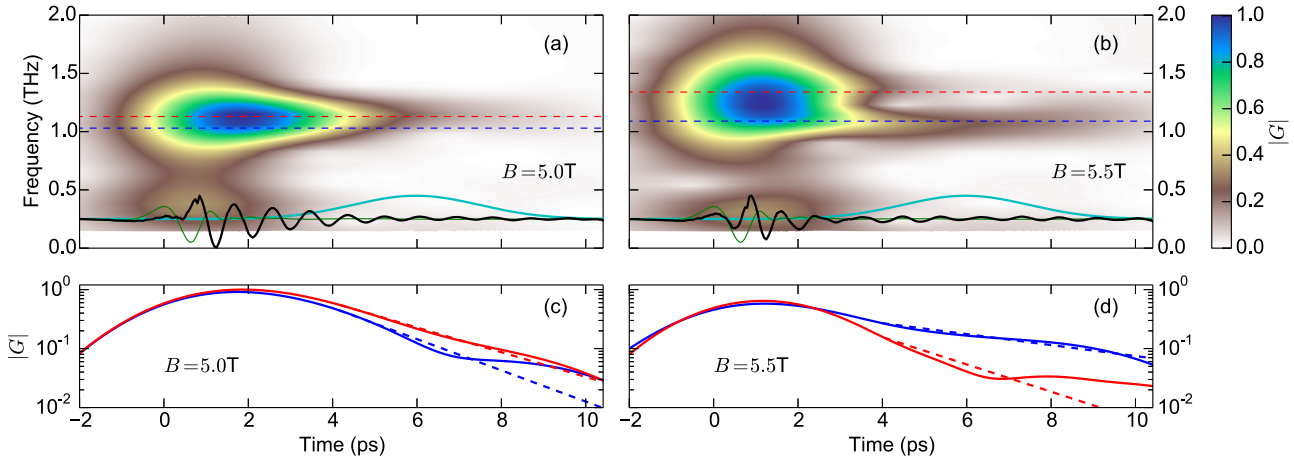

FIG. 2. (Color online) (a) Time- and frequency-resolved cyclotron amplitude $|G(\omega,t')|$ obtained from the Gabor-Morlet transform [Eq. (1), $\sigma = 1.5$ ps] for SiGe1 at 2 K and $B = 5.0$ T. Dark blue shading indicates $|G| = 1$ (see color bar, right). The incident electric field $E(B = 0)$ (thin, green line), induced change $E(B) - E(B = 0)$ (thick, black line), and an example of the Gaussian time window (blue line, $t' = 6.0$ ps) are also shown. (b) As (a), for $B = 5.5$ T. (c) $|G|$ versus time at two frequencies, shown by the blue and red dashed lines in (a). Solid lines are from experiment; dashed lines show single-exponential decays with lifetimes 1.6 ps (blue) and 2.1 ps (red). (d) as (c), but for $B = 5.5$ T, and with lifetimes 4.7 ps (blue) and 1.9 ps (red).

τ_t determined for SiGe1 and SiGe2. However, this short τ_s is not consistent with our observation of interference between spin-up-up and spin-down-down CRs, which show that $\tau_s >$ 10 ps. The DP mechanism, which is significant only in the case of strong momentum scattering [30], therefore does not dominate in our samples. In bulk Ge, where the EY mechanism dominates, $\tau_s \simeq 150$ ps for holes at 6 K [31].

Fits to ΔE in the time domain, shown in Fig. 1(a) by the black dashed lines, were utilized to extract the lifetimes τ_i, spin-split subband densities p_i, and CR frequencies $\omega_{c,i}$ for each resonance i. The time-domain fits in Fig. 1(a) used the formalism presented in Ref. [25], also given in the Supplemental Material [22], where the equivalence to a quantum (Bloch equation) approach [32] is also shown. Two contributions are considered even where the split is not resolved in the frequency domain because of a better agreement with time-domain data [22] and because time slices of the Gabor-Morlet transform show a nonexponential decay [as described above with reference to Fig. 2(c)]. The transmission $|T(\omega,B)|$ calculated for each heterostructure is reported in Fig. 1(b), where parameters obtained from the time domain, for $B \leqslant 6$ T, were used. At $B \geqslant 4$ T the increased energy separation of the observed CRs permitted fitting in the frequency domain.

The fitted p_i were averaged over $1 \leqslant B \leqslant 3$ T giving $p_1 = 5.2 \pm 0.2 \times 10^{11}\,\mathrm{cm}^{-2}$ and $p_2 = 4.5 \pm 0.2 \times 10^{11}\,\mathrm{cm}^{-2}$ for SiGe1, $p_1 = 1.6 \pm 0.3 \times 10^{11}\,\mathrm{cm}^{-2}$ and $p_2 = 1.5 \pm 0.3 \times 10^{11}\,\mathrm{cm}^{-2}$ for SiGe2. These values were used to get $p = p_1 + p_2$, as reported in Table I, and correspond to spin polarizations $p_1 - p_2/(p_1 + p_2)$ of 7% for SiGe1 and 3% for SiGe2. At these densities only the ground-state heavy-hole subband is occupied at 2 K. The heavy-hole effective mass was determined by a linear fit of the CR frequencies for $B \leqslant 3$ T to be $m^* = 0.115 \pm 0.003\ m_0$ and $0.083 \pm 0.005\ m_0$ for SiGe1 and SiGe2, respectively. The increased effective mass of SiGe1 in comparison to SiGe2 (lower p) is a consequence of nonparabolicity [33] and is discussed in more detail below.

In QWs with structural inversion asymmetry Landau levels have energies $E_N^{\pm}$ that depend on the combined influence of the Zeeman effect and Rashba spin-orbit coupling, and are given by

$$E_N^{\pm} = \hbar\omega_c\left(N + \frac{1}{2} \pm m_J\right) \mp m_J\sqrt{(\hbar\omega_c - g^*\mu_B B)^2 + \frac{eB}{\pi\hbar p}\Delta^2\left(N + \frac{1}{2} \pm m_J\right)}, \tag{2}$$

where $m_J = \pm 3/2$ for heavy holes. This expression was derived assuming lowest-order spin-orbit interaction for HHs only [19], under the further constraint that the Zeeman energy is $E^{\pm}_{\mathrm{Zeeman}} = \pm m_J g^* \mu_B B$ when $\Delta = 0$.

Strong cyclotron resonance absorption is permitted between adjacent Landau levels ($\Delta N = \pm 1$) with the same spin state ($\Delta m_J = 0$), and with energies $E^{\pm}_{\mathrm{cr}} = E^{\pm}_{N+1} - E^{\pm}_N$ that can be calculated from Eq. (2). Without Rashba spin-orbit coupling ($\Delta = 0$), the Zeeman splitting of Landau levels does not lead to spin-split CR energies $E^{\pm}_{\mathrm{cr}}$ for a *parabolic* band. In a *nonparabolic* band at a sufficiently high chemical potential μ both m^* and g^* can differ between adjacent Landau levels. This leads to the Zeeman splitting of the cyclotron resonance, as witnessed for $B > 8$ T by Engelhardt *et al.* [34] in sGe-QW 2DHG structures at 1.5 K. No clear spin-split peaks were reported at lower magnetic fields [34] in the region where Zeeman splitting and band nonparabolicity are less significant, due to the lower Hall mobility μ_{H} of the samples ($\mu_{\mathrm{H}} = 1.5 \times 10^4\,\mathrm{cm}^2/\mathrm{V\ s}$ [34] in comparison with $\mu_{\mathrm{H}} > 4.5 \times 10^5\,\mathrm{cm}^2/\mathrm{V\ s}$ herein; see Table II).

Although the chemical potential is low in the samples studied herein, in sGe-QWs the HH subband dispersion is highly nonparabolic owing to the interaction with the LH and SO bands [19]. Nonparabolicity was taken into account in Eq. (2) using the Kane ($\mathbf{k}\cdot\mathbf{p}$) model [35] to include the

TABLE II. Cubic Rashba coefficients and energy splitting evaluated from (i) the magnetic-field dependence of the cyclotron splitting energy (β, Δ), (ii) the spin-resolved subband densities (β_p, Δ_p), and (iii) SdH oscillations ($\beta_{\rm MT}$) [23]. Magnetotransport results for the quantum lifetime ($\tau_{\rm q}$), transport lifetime ($\tau_{\rm t,MT}$), and the transport lifetime obtained from THz-TDS ($\tau_{\rm t}$) (see text) are also given.

	β (10^{-28} eV m^3)	Δ (meV)	β_p (10^{-28} eV m^3)	Δ_p (meV)	$\beta_{\rm MT}$ (10^{-28} eV m^3)	$\tau_{\rm q}$ (ps)	$\tau_{\rm t,MT}$ (ps)	$\tau_{\rm t}$ (ps)
SiGe1	0.5 ± 0.1	1.6 ± 0.2	0.9 ± 0.3	2.8 ± 0.8	1.0 ± 0.6	0.5	24	31 ± 1
SiGe2	1.2 ± 0.4	0.6 ± 0.2	1.2	0.6	[a]	1.6,1.4,0.87[b]	29	33 ± 3

[a]A contribution from the B:SiGe supply layer prevented the determination of $\beta_{\rm MT}$ from an analysis of SdH oscillations.
[b]SdH oscillations revealed carriers with different τ_q.

energy dependence of g^* and m^*, which differ from the band edge values of g_0 and m_b^* as described in the Supplemental Material [22].

In Figs. 3(a) and 3(b) the calculated Landau level energies are reported for SiGe1 and SiGe2. The modeled $E_{\rm cr}^{\pm}$ are in excellent agreement with the experimental CR frequencies, as shown in Figs. 3(c) and 3(d). Both Rashba and Zeeman splitting effects were required to model the full range of magnetic fields for both samples. The energy splitting Δ was found to be 1.6 ± 0.2 meV for SiGe1 and 0.6 ± 0.2 meV for SiGe2. Best fit at high B required a nonparabolicity factor $\alpha_{\rm NP} = 3 \times 10^{-5}\,{\rm eV}^{-1}$ for both samples, with $g_0 = 3.2$ for SiGe1 and $g_0 = 7.0$ for SiGe2. These are in line with the value of $g^* = 4.3$ reported for a 15-nm-thick Ge-QW [36], and with the expectation that g increases in magnitude for wider wells as the bulk limit is approached [19]. The fitted band masses were $m_b^* = 0.103\, m_0$ for SiGe1 and $0.087\, m_0$ for SiGe2.

For the cubic Rashba interaction the in-plane hole energy is given by $E_{\parallel}^{\pm} = ak_{\parallel}^2 \pm \beta k_{\parallel}^3$ for in-plane wave vector $k_{\parallel}$, where $a = \hbar^2/2m^*$ and β is the Rashba spin-orbit coefficient. Only the HH subband is populated, and therefore only the cubic Rashba effect contributes to the splitting energy $\Delta = |E_{\parallel}^{+} - E_{\parallel}^{-}| = 2\beta k_{\parallel}^3$ of holes in strained Ge-QWs [21]. The cubic Rashba coefficient β can be determined by considering $k_{\parallel} \simeq k_{\rm F} = \sqrt{2\pi p}$, where $k_{\rm F}$ is the Fermi wave vector, as the HH energy is close to μ. This leads to $\beta = 0.5 \pm 0.1 \times 10^{-28}\,{\rm eV\,m^3}$ and $1.2 \pm 0.4 \times 10^{-28}\,{\rm eV\,m^3}$ for SiGe1 and SiGe2, respectively.

As an alternative means to calculate the cubic Rashba coefficients the spin-split subband densities p_1, p_2 obtained from THz-TDS can be utilized. The required expression [19] is

$$\beta_p = \sqrt{\frac{2}{\pi}}\,\frac{\hbar^2}{2m^*}\,\frac{p(p_+^* - p_-^*) + \Delta p(p_+^* + p_-^*)}{6p^2 + 2(\Delta p)^2}, \qquad (3)$$

where $p = p_1 + p_2$, $\Delta p = |p_2 - p_1|$, and $p_{\pm}^* = \sqrt{p \pm \Delta p}$. Performing this analysis (using the hole densities and values of $m^* = m_{\rm THz}^*$ reported above and in Table I) results in $\beta_p = 0.9 \pm 0.3 \times 10^{-28}\,{\rm eV\,m^3}$ for SiGe1 and $1.2 \times 10^{-28}\,{\rm eV\,m^3}$ for SiGe2. These values, and the energy splitting Δ_p calculated from β_p, are in accord with values from the CR energies, as summarized in Table II.

Further evidence for the enhanced Rashba interaction in SiGe1 comes from device magnetotransport at $B \leqslant 2$ T, where two spin-split subbands were evident in the Fourier spectrum of SdH oscillations [23]. From the determined subband densities a cubic Rashba coefficient $\beta_{\rm MT} = 1.0 \pm 0.6 \times 10^{-28}\,{\rm eV\,m^3}$ was obtained [23], in agreement with the values from THz-TDS (Table II). In SiGe2 a conductive pathway within the B:SiGe supply layer complicated the

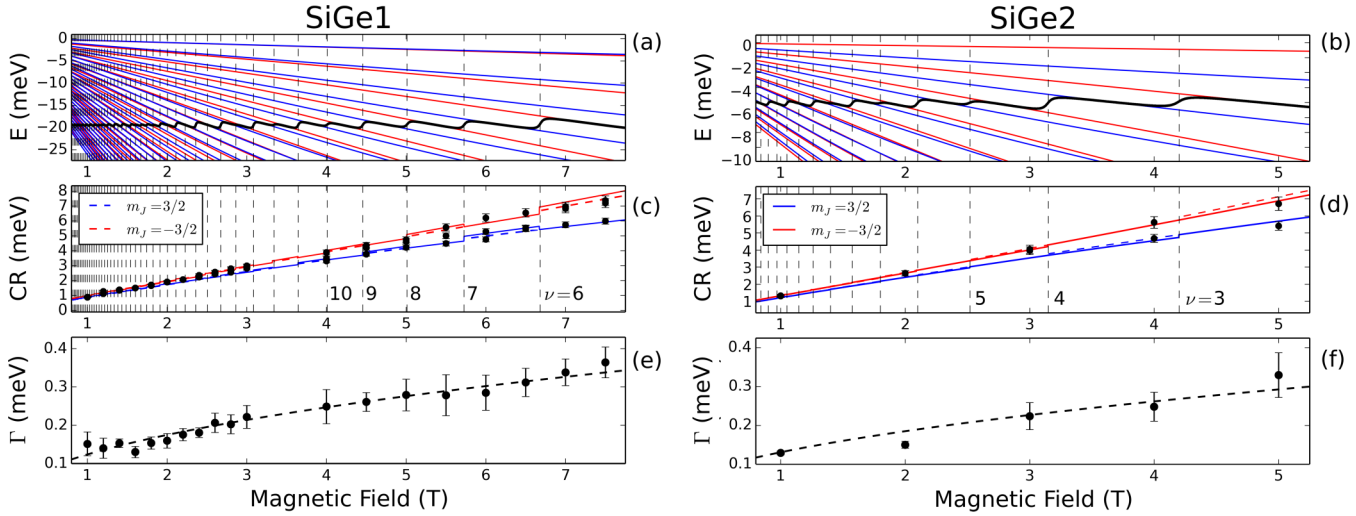

FIG. 3. (Color online) (a), (b) Heavy-hole Landau levels for SiGe1 and SiGe2, respectively, calculated from Eq. (2) with parameters as described in the text. The black dashed vertical lines are the magnetic field values for which the filling factor ν is an integer, while the black line describes the evolution of the chemical potential μ with the magnetic field. (c), (d) Calculated (lines) and experimental (points) cyclotron frequencies for transitions between spin up ($m_J = 3/2$, blue lines) and spin down ($m_J = -3/2$, red lines) states. (e), (f) Landau level width $\Gamma = \hbar/\tau_{\rm THz}$ obtained from experiment (points). The dashed black line is a fit using $\Gamma \propto \sqrt{B}$ (see text).

SdH spectra [37] and prevented the determination of β_{MT}. Results from THz time-domain cyclotron spectroscopy were not influenced by holes in the supply layer (which have higher m^* than holes in the QW [38]). The strong increase in β reported here for SiGe1 and SiGe2 in comparison to Ref. [21] ($\beta \leqslant 0.1 \times 10^{-28}$ eV m^3) can be attributed to the lower strain used in the present study (0.8% instead of 2.1%). The reduced strain leads to a ~2.75 times smaller HH-LH energy splitting (~40 meV instead of ~110 meV in Ref. [21]) [38]. Using $\beta \propto 1/(E_{HH} - E_{LH})^2$ for the Rashba coefficient's dependence on HH-LH splitting [21,30], this leads to an approximately 8-fold increase in β, in reasonable agreement with the observed values.

The CR absorption linewidth measures the energetic width of the Landau levels closest to the chemical potential, and can be used to deduce scattering times and mechanisms. The CR linewidths $\Gamma = \hbar/\tau_{THz}$ at different B are shown in Figs. 3(e) and 3(f) for SiGe1 and SiGe2, respectively. Here, the lifetimes reported are the average of spin-up-up and spin-down-down CR lifetimes, which varied by up to 10% at each B according to both time-domain fits and the Gabor-Morlet amplitude $|G(\omega,t')|$ at the resonance frequencies. A variation in lifetime for different transitions can result for instance from the partial occupation of a LL, as pictured in Fig 1(d). The measured values of τ_{THz} (averaged over spin-up-up and spin-down-down transitions) decrease monotonically from around 5 ps at $B = 1.0$ T to 2 ps above $B = 5$ T, leading to an increase in Γ. The CR lifetimes are slightly larger than single-particle (quantum) lifetimes τ_q obtained by analyzing Shubnikov–de Haas oscillations in the magnetoresistance [23,37], which are below 2 ps for both samples (Table II).

The experimental CR linewidth is consistent with $\Gamma \propto \sqrt{B}$, as indicated by the dashed lines in Figs. 3(e) and 3(f). For short-range scattering potentials $\Gamma = \sqrt{2\hbar^2 eB/\pi m_b^* \tau_t}$, where τ_t is the $B = 0$ transport relaxation time [9]. Using the experimental Γ and m_b^* the zero-field lifetimes were found to be $\tau_t = 31 \pm 1$ ps and 33 ± 3 ps for SiGe1 and SiGe2, respectively. These are in line with $\tau_{t,MT}$ obtained from the dc Hall mobility (Table II). CR lifetime broadenings of the order of 0.3 meV (as reported herein) and with the same $\Gamma \propto \sqrt{B}$ dependence can arise from hole-acoustic phonon scattering mediated by the deformation potential [39–41]. Interface roughness scattering and remote and background ionized impurity scattering are also thought to contribute to the mobility of Ge-QWs [42]. Both transport lifetimes $\tau_{t,MT}$ and τ_t were substantially greater than τ_q (Table II). Both remote ionized impurity scattering and interface roughness scattering can result in $\tau_{t,MT} > \tau_q$ [43].

In conclusion, narrow cyclotron resonances of spin-split heavy hole states were observed in strained Ge quantum wells. The Rashba splitting energy for holes in strained Ge quantum wells ($\Delta \sim 2.0$ meV) was found to be enhanced in comparison to previous reports, and approaches values found for 2DEGs in III-V semiconductors (e.g., $\Delta = 4.0$ meV in InAs QWs [44] and $\Delta = 11.6$ meV in GaN QWs [45]). Cyclotron energies and spin-split subband densities were used to independently estimate the Rashba coefficient. Importantly, the Rashba coefficient was obtained from THz time-domain cyclotron spectroscopy in a noncontact fashion and for a sample with a parallel conduction path (SiGe2), a challenge with device magnetotransport.

An enhanced spin-orbit interaction and a long spin decoherence time were demonstrated concurrently with a high mobility, emphasizing the potential of strain-engineered Ge quantum wells for CMOS-compatible spintronics. The experimental approach adopted herein is highly complementary to previous magnetotransport studies of the Rashba effect in Ge quantum wells [21,23] as it is contactless and therefore is not sensitive to device fabrication issues. Finally, the time-frequency decomposition method applied to data from THz time-domain spectroscopy permitted spin-split resonances to be identified even when their spacing in frequency was smaller than their linewidth.

The authors would like to thank Dr. M. B. Johnston for access to a superconducting magnet, and the EPSRC (UK) for financial support under Grants No. EP/H003444/2 and No. EP/J003263/1.

[1] T. Kimura, T. Goto, H. Shintani, K. Ishizaka, T. Arima, and Y. Tokura, Nature (London) **426**, 55 (2003).
[2] S. P. P. Jones, S. M. Gaw, K. I. Doig, D. Prabhakaran, E. M. Hétroy Wheeler, A. T. Boothroyd, and J. Lloyd-Hughes, Nat. Commun. **5**, 3787 (2014).
[3] M. König, S. Wiedmann, C. Brüne, A. Roth, H. Buhmann, L. W. Molenkamp, X.-L. Qi, and S.-C. Zhang, Science **318**, 766 (2007).
[4] J. Balakrishnan, G. Kok Wai Koon, M. Jaiswal, A. H. Castro Neto, and B. Özyilmaz, Nat. Phys. **9**, 284 (2013).
[5] F. J. Ohkawa and Y. Uemura, J. Phys. Soc. Jpn. **37**, 1325 (1974).
[6] H. L. Stormer, Z. Schlesinger, A. Chang, D. C. Tsui, A. C. Gossard, and W. Wiegmann, Phys. Rev. Lett. **51**, 126 (1983).
[7] S. Datta and B. Das, Appl. Phys. Lett. **56**, 665 (1990).
[8] H. C. Koo, J. H. Kwon, J. Eom, J. Chang, S. H. Han, and M. Johnson, Science **325**, 1515 (2009).
[9] T. Ando, A. B. Fowler, and F. Stern, Rev. Mod. Phys. **54**, 437 (1982).
[10] J. Lloyd-Hughes, J. Phys. D: Appl. Phys. **47**, 374006 (2014).
[11] S. M. Sze, *Physics of Semiconductor Devices*, 2nd ed. (Wiley-Blackwell, New York, 1981).
[12] B. Rössner, D. Chrastina, D. Isella, and H. G. von Känel, Appl. Phys. Lett. **84**, 3058 (2004).
[13] M. Myronov, K. Sawano, Y. Shiraki, T. Mouri, and K. M. Itoh, Appl. Phys. Lett. **91**, 082108 (2007).
[14] R. J. H. Morris, D. R. Leadley, R. Hammond, T. J. Grasby, T. E. Whall, and E. H. C. Parker, J. Appl. Phys. **96**, 6470 (2004).
[15] M. Myronov, D. Leadley, and Y. Shiraki, Appl. Phys. Lett. **94**, 092108 (2009).
[16] M. Myronov, C. Morrison, J. Halpin, S. Rhead, C. Casteleiro, J. Foronda, V. A. Shah, and D. Leadley, Jpn. J. Appl. Phys. **53**, 04EH02 (2014).

[17] M. Myronov, Y. Shiraki, T. Mouri, and K. Itoh, Appl. Phys. Lett. **90**, 192108 (2007).
[18] K. Sawano, K. Toyama, R. Masutomi, T. Okamoto, N. Usami, K. Arimoto, K. Nakagawa, and Y. Shiraki, Appl. Phys. Lett. **95**, 122109 (2009).
[19] R. Winkler, *Spin-Orbit Coupling Effects in Two-Dimensional Electron and Hole Systems* (Springer-Verlag, Berlin, 2003).
[20] R. Winkler, M. Merkler, T. Darnhofer, and U. Rössler, Phys. Rev. B **53**, 10858 (1996).
[21] R. Moriya, K. Sawano, Y. Hoshi, S. Masubuchi, Y. Shiraki, A. Wild, C. Neumann, G. Abstreiter, D. Bougeard, T. Koga *et al.*, Phys. Rev. Lett. **113**, 086601 (2014).
[22] See Supplemental Material at http://link.aps.org/supplemental/10.1103/PhysRevB.92.045303 for a description of the detector deconvolution, time-domain fits, and substrate cyclotron resonance.
[23] C. Morrison, M. Myronov, P. Wiśniewski, S. D. Rhead, J. Foronda, and D. R. Leadley, Appl. Phys. Lett. **105**, 182401 (2014).
[24] J. Lloyd-Hughes and T.-I. Jeon, J. Infrared, Millimeter, Terahertz Waves **33**, 871 (2012).
[25] D. Some and A. V. Nurmikko, Appl. Phys. Lett. **65**, 3377 (1994).
[26] X. F. Wang, D. J. Hilton, L. Ren, D. M. Mittleman, J. Kono, and J. L. Reno, Opt. Lett. **32**, 1845 (2007).
[27] G. Gallot, J. Q. Zhang, R. W. McGowan, T.-I. Jeon, and D. Grischkowsky, Appl. Phys. Lett. **74**, 3450 (1999).
[28] G. Dresselhaus, A. F. Kip, and C. Kittel, Phys. Rev. **98**, 368 (1955).
[29] I. Žutić and S. Das Sarma, Rev. Mod. Phys. **76**, 323 (2004).
[30] R. Winkler, D. Culcer, S. J. Papadakis, B. Habib, and M. Shayegan, Semicond. Sci. Technol. **23**, 114017 (2008).
[31] C. Hautmann, B. Surrer, and M. Betz, Phys. Rev. B **83**, 161203 (2011).
[32] T. Arikawa, X. Wang, D. J. Hilton, J. L. Reno, W. Pan, and J. Kono, Phys. Rev. B **84**, 241307 (2011).
[33] B. Rössner, G. Isella, and H. v. Knel, Appl. Phys. Lett. **82**, 754 (2003).
[34] C. Engelhardt, D. Többen, M. Aschauer, F. Schäffler, G. Abstreiter, and E. Gornik, Solid-State Electron. **37**, 949 (1994).
[35] J. Scriba, A. Wixforth, J. Kotthaus, C. Bolognesi, C. Nguyen, and H. Kroemer, Solid State Commun. **86**, 633 (1993).
[36] I. B. Berkutov, V. V. Andrievski, Y. F. Komnik, O. A. Mironov, M. Mironov, and D. R. Leadley, Low Temp. Phys. **35**, 141 (2009).
[37] C. Morrison, M. Myronov, C. P. Casteleiro, and D. R. Leadley (unpublished).
[38] M. V. Fischetti and S. E. Laux, J. Appl. Phys. **80**, 2234 (1996).
[39] M. Singh, Phys. Rev. B **36**, 5062 (1987).
[40] M. Singh, Phys. Rev. B **36**, 1178 (1987).
[41] M. P. Chaubey, Phys. Rev. B **38**, 5422 (1988).
[42] A. H. A. Hassan, R. J. H. Morris, O. A. Mironov, R. Beanland, D. Walker, S. Huband, A. Dobbie, M. Myronov, and D. R. Leadley, Appl. Phys. Lett. **104**, 132108 (2014).
[43] T. Unuma, M. Yoshita, and T. Noda, J. Appl. Phys. **93**, 1586 (2003).
[44] J. Luo, H. Munekata, F. F. Fang, and P. J. Stiles, Phys. Rev. B **41**, 7685 (1990).
[45] K. S. Cho, T.-Y. Huang, H.-S. Wang, M.-G. Lin, T.-M. Chen, C.-T. Liang, Y. F. Chen, and I. Lo, Appl. Phys. Lett. **86**, 222102 (2005).